

EXCLUSIVE TWO-PHOTON PROCESSES IN QCD*

STANLEY J. BRODSKY

Stanford Linear Accelerator Center
Stanford University, Stanford, California 94309, USA*(Received January 2, 2006)*

Hadron pair production from two-photon annihilation plays an important role in unraveling the perturbative and non-perturbative structure of QCD, first by testing the validity and empirical applicability of leading-twist factorization theorems, second by verifying the structure of the underlying perturbative QCD subprocesses, and third, through measurements of angular distributions and ratios which are sensitive to the shape of the distribution amplitudes. In effect, photon–photon collisions provide a microscope for testing fundamental scaling laws of PQCD and for measuring distribution amplitudes. The determination of the shape and normalization of the distribution amplitude is particularly important in view of their importance in the analysis of exclusive semi-leptonic and two-body hadronic B -decays. The data from the Belle and CLEO collaborations on single and double meson production are in excellent agreement with the QCD predictions. In contrast, the normalization of the nominal leading-order predictions of PQCD for proton pair production appears to be significantly below recent Belle measurements. I also review issues relating to renormalization scale setting.

PACS numbers: 12.38.-t, 13.66.Bc, 13.40.-f, 13.66.Lm

1. Introduction

Photon–photon collisions provide a comprehensive laboratory for testing the fundamental couplings and dynamics of the Standard Model and beyond [1]. In particular, two-photon exclusive processes such as $\gamma\gamma \rightarrow \pi^+\pi^-$, $\gamma\gamma \rightarrow p\bar{p}$, and $\gamma\gamma^* \rightarrow \pi^0$ provide a remarkable window into hadron dynamics and structure and recent measurements utilizing the virtual photon beams of e^+e^- colliders are now providing detailed tests of QCD.

At large momentum transfer, the angular distribution of hadron pairs produced by photon–photon annihilation are among the best determinants

* Presented at the PHOTON2005 Conference, 31 August–4 September 2005, Warsaw, Poland.

of the shape of the meson and baryon distribution amplitudes $\phi_M(x, Q)$, and $\phi_B(x_i, Q)$ which control almost all exclusive processes involving a hard scale Q . The determination of the shape and normalization of the distribution amplitudes, which are gauge-invariant and process-independent measures of the valence wavefunctions of the hadrons, has become particularly important in view of their importance in the analysis of exclusive semi-leptonic and two-body hadronic B -decays [2–6]. There has also been considerable progress both in calculating hadron wavefunctions from first principles in QCD and in measuring them using diffractive di-jet dissociation.

2. The photon-to-pion transition form factor and the pion distribution amplitude

The simplest and perhaps most elegant illustration of an exclusive reaction in QCD is the evaluation of the photon-to-pion transition form factor $F_{\gamma \rightarrow \pi}(Q^2)$ which is measurable in single-tagged two-photon $ee \rightarrow ee\pi^0$ reactions and tests the transition from the anomaly-dominated pion decay constant to the short-distance structure of currents dictated by the operator-product expansion and perturbative QCD factorization theorems. The transition form factor is defined via the invariant amplitude $\Gamma^\mu = -ie^2 F_{\pi\gamma}(Q^2) \varepsilon^{\mu\nu\rho\sigma} p_\nu^\pi \varepsilon_\rho q_\sigma$. As in inclusive reactions, one must specify a factorization scheme which divides the integration regions of the loop integrals into hard and soft momenta, compared to the resolution scale \tilde{Q} . At leading twist, the transition form factor then factorizes as a convolution of the $\gamma^*\gamma \rightarrow q\bar{q}$ amplitude (where the quarks are collinear with the final state pion) with the valence light-cone wavefunction of the pion [7]:

$$F_{\gamma M}(Q^2) = \frac{4}{\sqrt{3}} \int_0^1 dx \phi_M(x, \tilde{Q}) T_{\gamma \rightarrow M}^H(x, Q^2). \quad (1)$$

The hard scattering amplitude for $\gamma\gamma^* \rightarrow q\bar{q}$ is

$$T_{\gamma M}^H(x, Q^2) = [(1-x)Q^2]^{-1} (1 + \mathcal{O}(\alpha_s)).$$

For the asymptotic distribution amplitude $\phi_\pi^{\text{asympt}}(x) = \sqrt{3}f_\pi x(1-x)$ one predicts [8]

$$Q^2 F_{\gamma\pi}(Q^2) = 2f_\pi \left(1 - \frac{5}{3} \frac{\alpha_V(Q^*)}{\pi} \right),$$

where $Q^* = e^{-3/2}Q$ is the estimated BLM scale for the pion form factor in the V scheme.

3. Non-perturbative calculations of the pion distribution amplitude

The distribution amplitude $\phi(x, \tilde{Q})$ is the gauge-invariant Fourier transform of the vacuum to meson matrix element $\langle 0 | \bar{q}(x)W(x, 0)q(0) | M \rangle$ where W is the Wilson line. It can be computed from the integral over transverse momenta of the renormalized hadron valence wavefunction in the light-cone gauge at fixed light-cone time [7]:

$$\phi(x, \tilde{Q}) = \int d^2 k_{\perp} \theta \left(\tilde{Q}^2 - \frac{k_{\perp}^2}{x(1-x)} \right) \psi^{(\tilde{Q})}(x, k_{\perp}), \quad (2)$$

where a global cutoff in invariant mass is identified with the resolution \tilde{Q} . The distribution amplitude $\phi(x, \tilde{Q})$ is boost and gauge invariant and evolves in $\ln \tilde{Q}$ through an evolution equation [7]. Since it is formed from the same product of operators as the non-singlet structure function, the anomalous dimensions controlling $\phi(x, Q)$ dependence in the ultraviolet $\log Q$ scale are the same as those which appear in the DGLAP evolution of structure functions [9]. The decay $\pi \rightarrow \mu\nu$ normalizes the wave function at the origin: $\int_0^1 dx \phi(x, Q) = f_{\pi}/(2\sqrt{3})$. One can also compute the distribution amplitude from the gauge invariant Bethe–Salpeter wavefunction at equal light-cone time. This also allows contact with both QCD sum rules [10] and lattice gauge theory; for example, moments of the pion distribution amplitudes have been computed successfully in lattice gauge theory [11–14]. Conformal symmetry can be used as a template to organize the renormalization scales and evolution of QCD predictions [9, 15]. For example, Braun and collaborators have shown how one can use conformal symmetry to classify the eigensolutions of the baryon distribution amplitude [16].

Dalley [17] and Burkardt and Seal [18] have calculated the pion distribution amplitude from QCD using a combination of the discretized light-cone quantization [19] method for the x^- and x^+ light-cone coordinates with the transverse lattice method [20, 21] in the transverse directions. A finite lattice spacing a can be used by choosing the parameters of the effective theory in a region of renormalization group stability to respect the required gauge, Poincaré, chiral, and continuum symmetries. The overall normalization gives $f_{\pi} = 101$ MeV compared with the experimental value of 93 MeV. Figure 1(a) compares the resulting DLCQ/transverse lattice pion wavefunction with the best fit to the diffractive di-jet data (see the next section) after corrections for hadronization and experimental acceptance [22]. The theoretical curve is somewhat broader than the experimental result. However, there are experimental uncertainties from hadronization and theoretical errors introduced from finite DLCQ resolution, using a nearly massless

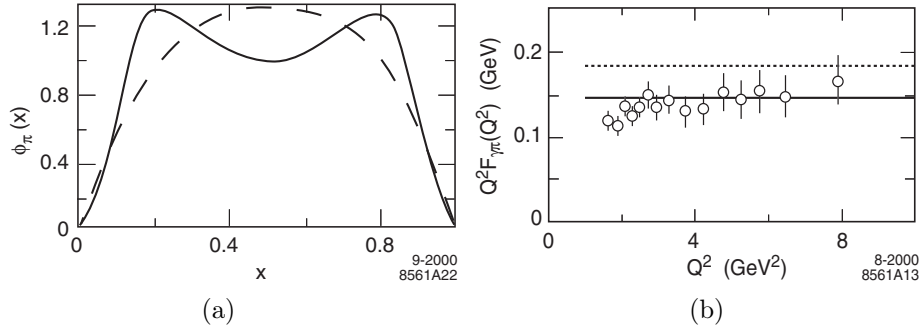


Fig. 1. (a) Transverse lattice results for the pion distribution amplitude at $Q^2 \sim 10 \text{ GeV}^2$. The solid curve is the theoretical prediction from the combined DLCQ/transverse lattice method [17]; the chain line is the experimental result obtained from dijet diffractive dissociation [22, 24]. Both are normalized to the same area for comparison. (b) Scaling of the transition photon to pion transition form factor $Q^2 F_{\gamma\pi^0}(Q^2)$. The dotted and solid theoretical curves are the perturbative QCD prediction at leading and next-to-leading order, respectively, assuming the asymptotic pion distribution. The data are from the CLEO collaboration [25].

pion, ambiguities in setting the factorization scale Q^2 , as well as errors in the evolution of the distribution amplitude from 1 to 10 GeV^2 . Instanton models also predict a pion distribution amplitude close to the asymptotic form [23]. Recent preliminary lattice gauge theory results for the second moment [11] are however somewhat broader than predicted by the asymptotic form. Bethe–Salpeter wavefunctions can also be used to predict light-cone wavefunctions and hadron distribution amplitudes by integrating over the relative k^- momentum. One can also use the Bethe–Salpeter wavefunctions within light-cone gauge quantized QCD [26, 27] in order to properly match to the light-cone gauge Fock state decomposition.

Recently Guy de Teramond and I have shown how one can use the AdS/CFT correspondence to obtain predictions for the light-front wavefunctions and distribution amplitudes of hadrons in a conformal approximation of QCD [28]. The prediction is consistent with the asymptotic form obtained in pQCD.

The E791 collaboration at Fermilab has measured the diffractive di-jet dissociation of 500 GeV incident pions on nuclear targets [22]. The results are consistent with color transparency, and the momentum partition of the jets conforms closely with the shape of the asymptotic distribution amplitude, $\phi_\pi^{\text{asympt}}(x) = \sqrt{3}f_\pi x(1-x)$, corresponding to the leading anomalous dimension solution of the ERBL QCD evolution equation [7, 29].

The pQCD predictions have been tested in measurements of $e\gamma \rightarrow e\pi^0$ by the CLEO collaboration [25] (see Fig. 1(b)). The flat scaling of the

$Q^2 F_{\gamma\pi}(Q^2)$ data from $Q^2 = 2$ to $Q^2 = 8$ GeV² provides an important confirmation of the applicability of leading twist QCD to this process. The magnitude of $Q^2 F_{\gamma\pi}(Q^2)$ is remarkably consistent with the predicted form, assuming the asymptotic distribution amplitude and including the LO QCD radiative correction with $\alpha_V(e^{-3/2}Q)/\pi \simeq 0.12$ in the V scheme [8]. Radyushkin [30, 31] and Kroll [32] have also noted that the scaling and normalization of the photon to pion transition form factor tends to favor the asymptotic form for the pion distribution amplitude and rules out broader distributions such as the two-humped form suggested by QCD sum rules [33]. When both photons are virtual, the denominator of T_H for the $\gamma\gamma^* \rightarrow \pi^0$ reaction becomes $(1-x)Q_1^2 + xQ_2^2$, and the amplitude becomes nearly insensitive to the shape of the distribution amplitude once it is normalized to the pion decay constant. Thus the ratio of singly virtual to doubly virtual pion production is particularly sensitive to the shape of $\phi_\pi(x, Q^2)$ since higher order corrections and normalization errors tend to cancel in the ratio.

4. Exclusive two-photon annihilation into hadron pairs

Two-photon reactions, $\gamma\gamma \rightarrow H\bar{H}$ at large $s = (k_1 + k_2)^2$ and fixed θ_{cm} , provide a particularly important laboratory for testing QCD since these cross-channel ‘‘Compton’’ processes are the simplest calculable large-angle exclusive hadronic scattering reactions. The helicity structure, and often even the absolute normalization can be rigorously computed for each two-photon channel [34]. In the case of meson pairs, dimensional counting [35] predicts that for large s , $s^4 d\sigma/dt(\gamma\gamma \rightarrow M\bar{M})$ scales at fixed t/s or θ_{cm} modulo logarithms from the running coupling of α_s and the evolution of the distribution amplitudes. The angular dependence of the $\gamma\gamma \rightarrow H\bar{H}$ amplitudes can be used to determine the shape of the process-independent distribution amplitudes, $\phi_H(x, Q)$. An important feature of the $\gamma\gamma \rightarrow M\bar{M}$ amplitude for meson pairs is that the contributions of Landshoff pitch singularities are power-law suppressed at the Born level — even before taking into account Sudakov form factor suppression. There are also no anomalous contributions from the $x \rightarrow 1$ endpoint integration region. Thus, as in the calculation of the meson form factors, each fixed-angle helicity amplitude can be written to leading order in $1/Q$ in the factorized form [$Q^2 = p_T^2 = tu/s$; $\tilde{Q}_x = \min(xQ, (1-x)Q)$]:

$$\mathcal{M}_{\gamma\gamma \rightarrow M\bar{M}} = \int_0^1 dx \int_0^1 dy \phi_{\bar{M}}(y, \tilde{Q}_y) T_H(x, y, s, \theta_{\text{cm}}) \phi_M(x, \tilde{Q}_x), \quad (3)$$

where T_H is the hard-scattering amplitude $\gamma\gamma \rightarrow (q\bar{q})(q\bar{q})$ for the production of the valence quarks collinear with each meson, and $\phi_M(x, \tilde{Q})$ is the ampli-

tude for finding the valence q and \bar{q} with light-cone fractions of the meson's momentum, integrated over transverse momenta $k_{\perp} < \tilde{Q}$. The contribution of non-valence Fock states are power-law suppressed. Furthermore, the helicity-selection rules [36] of perturbative QCD predict that vector mesons are produced with opposite helicities to leading order in $1/Q$ and all orders in α_s . The dependence in x and y of several terms in $T_{\lambda,\lambda'}$ is quite similar to that appearing in the meson's electromagnetic form factor. Thus much of the dependence on $\phi_M(x, Q)$ can be eliminated by expressing it in terms of the meson form factor. In fact, the ratio of the $\gamma\gamma \rightarrow \pi^+\pi^-$ and $e^+e^- \rightarrow \mu^+\mu^-$ amplitudes at large s and fixed θ_{CM} is nearly insensitive to the running coupling and the shape of the pion distribution amplitude:

$$\frac{\frac{d\sigma}{dt}(\gamma\gamma \rightarrow \pi^+\pi^-)}{\frac{d\sigma}{dt}(\gamma\gamma \rightarrow \mu^+\mu^-)} \sim \frac{4|F_{\pi}(s)|^2}{1 - \cos^2\theta_{\text{cm}}}. \quad (4)$$

The comparison of the pQCD prediction for the sum of $\pi^+\pi^-$ plus K^+K^- channels with Belle and CLEO data [37, 38] is shown in Fig. 2. The data for charged pion and kaon pairs show a clear transition to the scaling and angular distribution predicted by pQCD [34] for $W = \sqrt{s_{\gamma\gamma}} > 2$ GeV.

Unlike predictions based on the handbag approximation [39], there is a strong suppression of neutral pair production in pQCD due to the destructive interference of the $\sum_i e_i^2$ diagrams where the photons couple to a single quark line *versus* $\sum_{i \neq j} e_i e_j$ diagrams involving both quark currents. It is thus very important to measure the magnitude and angular dependence of the two-photon production of neutral pions and $\rho^+\rho^-$ in view of the strong sensitivity of these channels to the shape of meson distribution amplitudes (see Figs. 3 and 4). QCD also predicts that the production cross section for charged ρ -pairs (with any helicity) is much larger than for that of neutral ρ pairs, particularly at large θ_{cm} angles. Similar predictions are possible for other helicity-zero mesons.

There are several features of QCD which are required to ensure the consistency of the pQCD approach: (a) the effective QCD coupling $\alpha_s(Q^2)$ needs to be under control at the relevant scales of B decay; (b) the distribution amplitudes of the hadrons need to satisfy convergence properties at the endpoints; and (c) one requires the coherent cancellation of the couplings of soft gluons to color-singlet states. This property, color transparency [40], is a fundamental coherence property of gauge theory and leads to diminished final-state interactions and corrections to the pQCD factorizable contributions. The problem of setting the renormalization scale of the coupling for exclusive amplitudes is discussed in [8].

The observed scaling of the Belle and CLEO data, like other hard exclusive reactions, reflects the near conformal behavior of QCD. This behavior

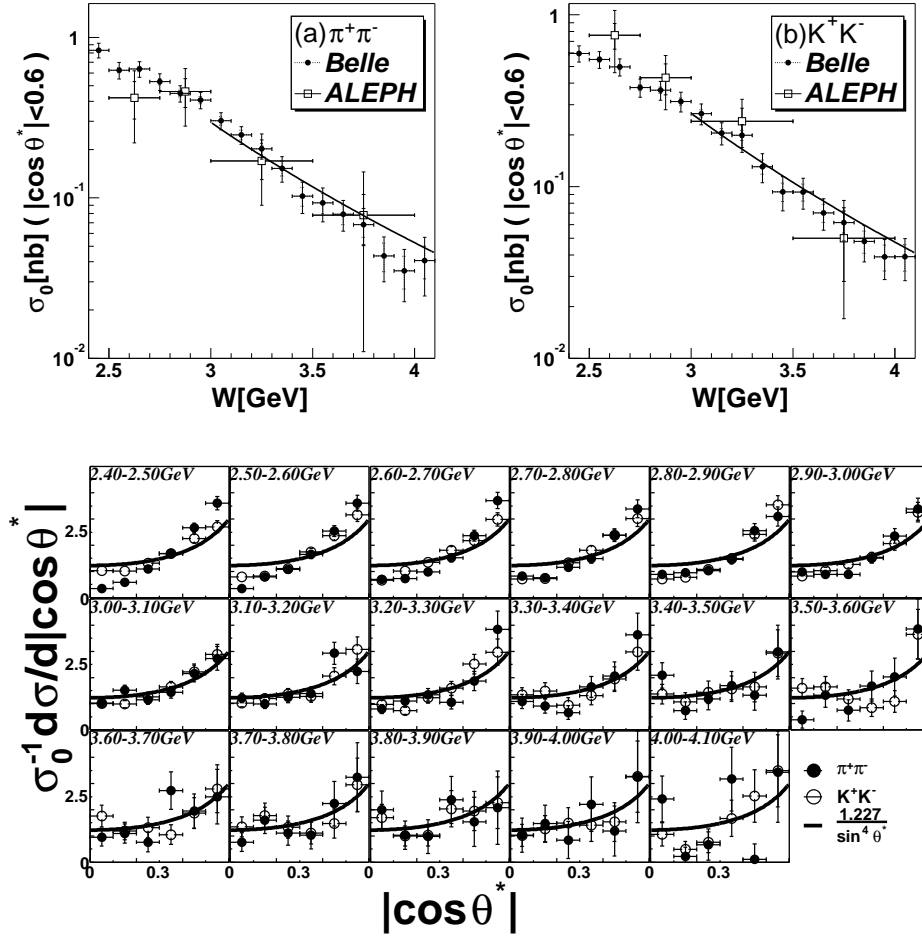


Fig. 2. Comparison of the sum of $\gamma\gamma \rightarrow \pi^+\pi^-$ and $\gamma\gamma \rightarrow K^+K^-$ meson pair production cross sections with the scaling and angular distribution of the perturbative QCD prediction [34]. The data are from the Belle and CLEO Collaborations [38].

can be understood if the QCD coupling $\alpha_s(Q^2)$ has an infrared fixed point; *i.e.*, constant behavior at small Q^2 . This also justifies the use of AdS/CFT to make predictions for QCD [41, 42]. Dimensional counting rules can be proven without the use of perturbation theory using AdS/CFT [41]. Theoretical and empirical evidence for an infrared fixed point is presented in Ref. [43–45].

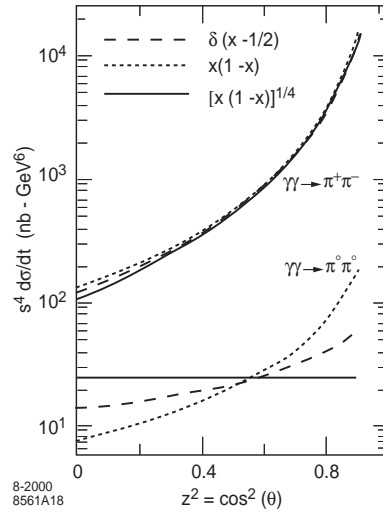


Fig. 3. Predictions for the angular distribution of the $\gamma\gamma \rightarrow \pi^+\pi^-$ and $\gamma\gamma \rightarrow \pi^0\pi^0$ pair production cross sections for three different pion distribution amplitudes [34].

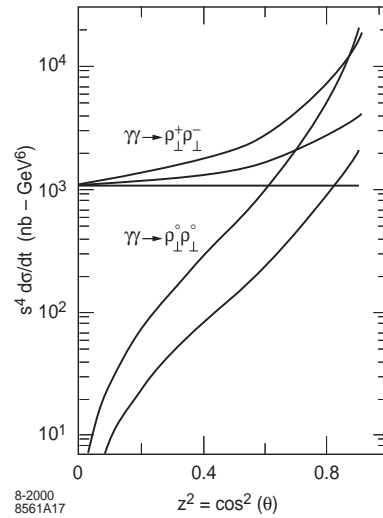


Fig. 4. Predictions for the angular distribution of the $\gamma\gamma \rightarrow \rho^+\rho^-$ and $\gamma\gamma \rightarrow \rho^0\rho^0$ pair production cross sections for three different ρ distribution amplitudes as in Fig. 3 [34].

5. Exclusive production of baryon pairs

Baryon pair production in two-photon annihilation is also an important testing ground for QCD since it is connected by crossing to Compton scattering and the deeply virtual Compton amplitudes which define generalized parton distributions as well as the polarization correction to the hyperfine splitting of hydrogen. The perturbative QCD predictions for the phase of the Compton amplitude phase can be tested in virtual Compton scattering by interference with Bethe–Heitler processes [46]. The Brooks–Dixon result could be used for $\gamma\gamma \rightarrow p\bar{p}$ by employing $t \rightarrow s$ crossing. The calculation of T_H for Compton scattering $\gamma p \rightarrow \gamma p$ requires the evaluation of 368 helicity-conserving tree diagrams which contribute to $\gamma(qqq) \rightarrow \gamma'(qqq)'$ at the Born level and a careful integration over singular intermediate energy denominators [47–49]. Brooks and Dixon [50] have recalculated the proton Compton process at leading order in pQCD, extending and correcting earlier work.

Recently the Belle collaboration [51] has made detailed measurements of the large angle $\gamma\gamma \rightarrow p\bar{p}$ cross section. (See Fig. 5.) The scaling of the data appears to be consistent with the leading-order pQCD prediction at $W = \sqrt{s_{\gamma\gamma}} > 3 \text{ GeV}$. However, the predicted normalization [52] appears to be too small compared to the data. This discrepancy is crucial to understand — it is possibly due to running coupling effects, higher order corrections, or the shape of the distribution amplitude. On the other hand, the prediction of the handbag [53] and the quark–diquark models [54] are much closer to

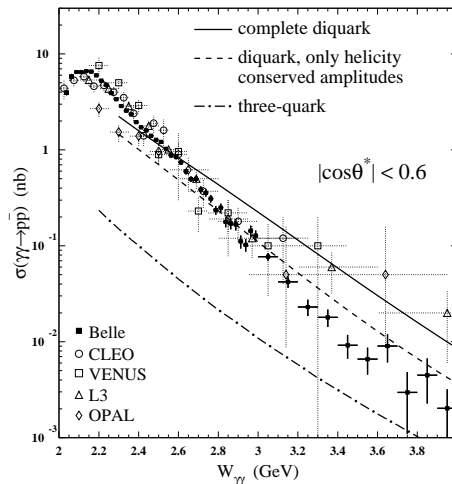


Fig. 5. Scaling of the $\gamma\gamma \rightarrow p\bar{p}$. The data is from the Belle and earlier experiments [51]. The three-quark prediction is the leading order QCD prediction from Farrar *et al.* [52]. The prediction of a quark–diquark model by Berger and Schweiger [54] is also shown.

the normalization of the Belle data [53] It is also useful to consider the ratio $d\sigma/dt(\gamma\gamma \rightarrow \bar{p}p)/d\sigma/dt(e^+e^- \rightarrow \bar{p}p)$ since the power-law fall-off, the normalization of the valence wavefunctions, and much of the uncertainty from the scale of the QCD coupling cancel. The scaling and angular dependence of this ratio is sensitive to the shape of the proton distribution amplitudes.

Pobylitsa *et al.* [55] have shown how the predictions of perturbative QCD can be extended to processes such as $\gamma\gamma \rightarrow p\bar{p}\pi$ where the pion is produced at low velocities relative to that of the p or \bar{p} by utilizing soft pion theorems in analogy to soft photon theorems in QED. The distribution amplitude of the $p\pi$ composite is obtained from the proton distribution amplitude from a chiral rotation. A test of this procedure in semi-inclusive electron scattering at large momentum transfer $ep \rightarrow p\pi$ and small invariant $p'\pi$ mass has been remarkably successful. Many other tests of the soft meson procedure are possible in multiparticle e^+e^- and $\gamma\gamma$ final states.

6. Scale-setting issues

The renormalization scale of the running coupling in processes such as the exclusive two-photon amplitudes can be set in QCD without ambiguity at each order in perturbation theory using the BLM method [8, 56]. The BLM scale is derived by incorporating the non-conformal terms associated with the β function into the argument of the running coupling. This can be done systematically using the skeleton expansion [15, 57]. The resulting scale at leading order is identical to the photon virtuality in QED applications and the gluon virtuality when one uses analogous physical schemes such as the pinch scheme and the α_V scheme. The BLM method properly sets the momentum scale so that flavor number is changed correctly in any scheme, including the $\overline{\text{MS}}$ scheme [58].

The scale determined by the BLM method is consistent with (a) the transitivity and other properties of the renormalization group [59], (b) the analytic Abelian limit at $N_C \rightarrow 0$ at fixed $C_F\alpha_s$, (c) relations between observables must be independent of the choice of intermediate renormalization scheme, and (d) the cut structure of amplitudes at the flavor thresholds. For example, consider the vacuum polarization lepton-loop correction to $e^+e^- \rightarrow e^+e^-$ in QED. The amplitude must be proportional to $\alpha(s)$ since this gives the correct cut of the forward amplitude at the lepton pair threshold $s = 4m_\ell^2$. Thus the renormalization scale $\mu_R^2 = s$ is exact and unambiguous in the conventional QED Goldberger–Low scheme. If one chooses any other scale $\mu_R^2 \neq s$, the scale $\mu_R^2 = s$ will be restored when one sums all bubble graphs.

It has been conventional to characterize pQCD predictions by using an arbitrary renormalization scale in the $\overline{\text{MS}}$ scheme, such as $\mu_R^2 = Q^2$, and

then varying the scale over an arbitrary range, *e.g.*, $Q^2/2 < \mu_R^2 < 2Q^2$ as a means to estimate the convergence of the perturbative series. However, the variation of μ_R^2 can only apply to the nonconformal terms, not the complete series. Furthermore, as noted above, one must set the scale appropriately so that amplitudes have the correct analytic cut structure at the quark thresholds. This is done correctly in any renormalization scheme by using the BLM method.

7. Other important two-photon QCD reactions

Two-photon annihilation $\gamma^*(q_1)\gamma^*(q_2) \rightarrow$ hadrons for real and virtual photons provide some of the most detailed and incisive tests of QCD.

Among the processes of special interest are:

1. The total two-photon annihilation hadronic cross section $\sigma(s, q_1^2, q_2^2)$, which is related to the light-by-light hadronic contribution to the muon anomalous moment.
2. The formation of $C = +$ hadronic resonances, which can reveal exotic states such as $q\bar{q}g$ hybrids and discriminate gluonium formation [60].
3. Hadron pair production processes involving virtual photons such as $\gamma^*\gamma \rightarrow \pi^+\pi^-, K^+K^-, p\bar{p}$, which at fixed invariant pair mass measures the $s \rightarrow t$ crossing of the virtual Compton amplitude [34]. When one photon is highly virtual, these exclusive hadron production channels are dual to the photon structure function $F_2^\gamma(x, Q^2)$ in the endpoint $x \rightarrow 1$ region at fixed invariant pair mass. The leading twist-amplitude for $\gamma^*\gamma \rightarrow \pi^+\pi^-$ is sensitive to the $1/x - 1/(1-x)$ moment of the $q\bar{q}$ distribution amplitude $\Phi_{\pi^+\pi^-}(x, Q^2)$ of the two-pion system [61, 62], the time-like extension of skewed parton distributions. In addition one can measure the pion charge asymmetry in $e^+e^- \rightarrow \pi^+\pi^-e^+e^-$ arising from the interference of the $\gamma\gamma \rightarrow \pi^+\pi^-$ Compton amplitude with the time-like pion form factor [63]. At the unphysical point $s = q_1^2 = q_2^2 = 0$, the amplitude is fixed by the low energy theorem to the hadron charge squared.
4. At fixed pair mass, and high photon virtuality, one can study the distribution amplitude of multi-hadron states [64].

A remarkable feature of the pQCD prediction for the Compton scattering amplitude $\gamma H \rightarrow \gamma H$ is the existence of a $J = 0$ fixed pole; *i.e.*, a constant term in the Regge expansion at high s at fixed t [65]. The result is also independent of the virtuality of the photons. This term reflects the local two-photon couplings of the two photons analogous to the seagull term in

scalar electrodynamics. It is also reflected in the angular distribution of the time-like processes $\gamma\gamma \rightarrow H\bar{H}$. The $J = 0$ fixed pole appears in vector meson pair production, but it does not appear, however, in the case of pseudoscalar meson pairs [34].

8. Conclusions

The leading-twist QCD predictions for exclusive two-photon processes such as the photon-to-pion transition form factor and $\gamma\gamma \rightarrow$ hadron pairs are based on rigorous factorization theorems. The data from the Belle and CLEO collaborations on $F_{\gamma\pi}(Q^2)$ and the sum of $\gamma\gamma \rightarrow \pi^+\pi^-$ and $\gamma\gamma \rightarrow K^+K^-$ channels are in excellent agreement with the QCD predictions. In contrast, the normalization of the nominal leading-order predictions of PQCD for proton pair production appears to be significantly below recent Belle measurements. It is particularly compelling to see a transition in angular dependence of the meson pair data between the low energy chiral and pQCD regimes. The success of leading-twist perturbative QCD scaling for these exclusive processes at presently experimentally accessible momentum transfer can be understood if the effective QCD coupling is approximately constant at the relatively small scales Q^* relevant to the hard scattering amplitudes [8]. The evolution of the quark distribution amplitudes in the low- Q^* domain also needs to be minimal. Sudakov suppression of the endpoint contributions is also strengthened if the coupling is frozen because of the exponentiation of a double logarithmic series. Evidence for an infrared fixed point is presented in Ref. [43–45].

Work supported by the Department of Energy under contract number DE-AC02-76SF00515.

REFERENCES

- [1] M. Krawczyk, *Eur. Phys. J.* **C33**, S638 (2004) [[hep-ph/0312341](#)].
- [2] A. Szczepaniak, E.M. Henley, S.J. Brodsky, *Phys. Lett.* **B243**, 287 (1990).
- [3] P. Ball, V.M. Braun, *Phys. Rev.* **D58**, 094016 (1998) [[hep-ph/9805422](#)].
- [4] M. Beneke, G. Buchalla, M. Neubert, C.T. Sachrajda, *Phys. Rev. Lett.* **83**, 1914 (1999) [[hep-ph/9905312](#)].
- [5] Y.Y. Keum, H.-n. Li, A.I. Sanda, *Phys. Lett.* **B504**, 6 (2001) [[hep-ph/0004004](#)].
- [6] Y.Y. Keum, H.-n. Li, A.I. Sanda, *Phys. Rev.* **D63**, 054008 (2001) [[hep-ph/0004173](#)].
- [7] G.P. Lepage, S.J. Brodsky, *Phys. Rev.* **D22**, 2157 (1980).

- [8] S.J. Brodsky, C.R. Ji, A. Pang, D.G. Robertson, *Phys. Rev.* **D57**, 245 (1998) [[hep-ph/9705221](#)].
- [9] S.J. Brodsky, Y. Frishman, G.P. Lepage, C.T. Sachrajda, *Phys. Lett.* **B91**, 239 (1980).
- [10] M.A. Shifman, A.I. Vainshtein, V.I. Zakharov, *Nucl. Phys.* **B147**, 448 (1979).
- [11] M. Gockeler *et al.*, [hep-lat/0510089](#).
- [12] G. Martinelli, C.T. Sachrajda, *Phys. Lett.* **B190**, 151 (1987).
- [13] D. Daniel, R. Gupta, D.G. Richards, *Phys. Rev.* **D43**, 3715 (1991).
- [14] L. Del Debbio, M. Di Pierro, A. Dougall, C.T. Sachrajda [UKQCD Collaboration], *Nucl. Phys. Proc. Suppl.* **83**, 235 (2000) [[hep-lat/9909147](#)].
- [15] S.J. Brodsky, E. Gardi, G. Grunberg, J. Rathsman, *Phys. Rev.* **D63**, 094017 (2001) [[hep-ph/0002065](#)].
- [16] V.M. Braun, S.E. Derkachov, G.P. Korchemsky, A.N. Manashov, *Nucl. Phys.* **B553**, 355 (1999) [[hep-ph/9902375](#)].
- [17] S. Dalley, *Nucl. Phys. Proc. Suppl.* **90**, 227 (2000) [[hep-ph/0007081](#)].
- [18] M. Burkardt, S.K. Seal, *Phys. Rev.* **D65**, 034501 (2002) [[hep-ph/0102245](#)].
- [19] H.C. Pauli, S.J. Brodsky, *Phys. Rev.* **D32**, 1993 (1985).
- [20] W.A. Bardeen, R.B. Pearson, E. Rabinovici, *Phys. Rev.* **D21**, 1037 (1980).
- [21] M. Burkardt, *Phys. Rev.* **D54**, 2913 (1996) [[hep-ph/9601289](#)].
- [22] D. Ashery [E791 Collaboration], [hep-ex/9910024](#).
- [23] V.Y. Petrov, V. Polyakov, R. Ruskov, C. Weiss, K. Goetze, *Phys. Rev.* **D59**, 114018 (1999) [[hep-ph/9807229](#)].
- [24] E.M. Aitala *et al.* [E791 Collaboration], *Phys. Rev. Lett.* **86**, 4768 (2001) [[hep-ex/0010043](#)].
- [25] J. Gronberg *et al.* [CLEO Collaboration], *Phys. Rev.* **D57**, 33 (1998) [[hep-ex/9707031](#)].
- [26] S.J. Brodsky, J.R. Hiller, D.S. Hwang, V.A. Karmanov, *Phys. Rev.* **D69**, 076001 (2004) [[hep-ph/0311218](#)].
- [27] P.P. Srivastava, S.J. Brodsky, *Phys. Rev.* **D61**, 025013 (2000) [[hep-ph/9906423](#)].
- [28] S.J. Brodsky, G.F. de Teramond, [hep-ph/0510240](#).
- [29] A.V. Efremov, A.V. Radyushkin, *Phys. Lett.* **B94**, 245 (1980).
- [30] A.V. Radyushkin, *Acta Phys. Pol. B* **26**, 2067 (1995) [[hep-ph/9511272](#)].
- [31] S. Ong, *Phys. Rev.* **D52**, 3111 (1995).
- [32] P. Kroll, M. Raulfs, *Phys. Lett.* **B387**, 848 (1996) [[hep-ph/9605264](#)].
- [33] V.L. Chernyak, A.R. Zhitnitsky, IYF-81-74
- [34] S.J. Brodsky, G.P. Lepage, *Phys. Rev.* **D24**, 1808 (1981).
- [35] S.J. Brodsky, G.R. Farrar, *Phys. Rev. Lett.* **31**, 1153 (1973).
- [36] S.J. Brodsky, G.P. Lepage, *Phys. Rev.* **D24**, 2848 (1981).
- [37] H. Nakazawa *et al.* [BELLE Collaboration], *Phys. Lett.* **B615**, 39 (2005) [[hep-ex/0412058](#)].

- [38] J. Dominick *et al.* [CLEO Collaboration], *Phys. Rev.* **D50**, 3027 (1994) [[hep-ph/9403379](#)].
- [39] M. Diehl, P. Kroll, C. Vogt, *Phys. Lett.* **B532**, 99 (2002) [[hep-ph/0112274](#)].
- [40] S.J. Brodsky, A.H. Mueller, *Phys. Lett.* **B206**, 685 (1988).
- [41] J. Polchinski, M.J. Strassler, *J. High Energy Phys.* **0305**, 012 (2003) [[hep-th/0209211](#)].
- [42] G.F. de Teramond, S.J. Brodsky, *Phys. Rev. Lett.* **94**, 201601 (2005) [[hep-th/0501022](#)].
- [43] L. von Smekal, A. Hauck, R. Alkofer, *Ann. Phys.* **267**, 1 (1998) [Erratum, *Ann. Phys.* **269**, 182 (1998)] [[hep-ph/9707327](#)].
- [44] S.J. Brodsky, S. Menke, C. Merino, J. Rathsmann, *Phys. Rev.* **D67**, 055008 (2003) [[hep-ph/0212078](#)].
- [45] S.J. Brodsky, [hep-ph/0408069](#).
- [46] S.J. Brodsky, F.E. Close, J.F. Gunion, *Phys. Rev.* **D6**, 177 (1972).
- [47] G.R. Farrar, H.-y. Zhang, *Phys. Rev. Lett.* **65**, 1721 (1990).
- [48] A.S. Kronfeld, B. Nizic, *Phys. Rev.* **D44**, 3445 (1991) [Erratum, *Phys. Rev.* **D46**, 2272 (1992)].
- [49] P.A.M. Guichon, M. Vanderhaeghen, *Prog. Part. Nucl. Phys.* **41**, 125 (1998) [[hep-ph/9806305](#)].
- [50] T.C. Brooks, L.J. Dixon, *Phys. Rev.* **D62**, 114021 (2000) [[hep-ph/0004143](#)].
- [51] C.C. Kuo *et al.*, *Phys. Lett.* **B621**, 41 (2005) [[hep-ex/0503006](#)].
- [52] G.R. Farrar, E. Maina, F. Neri, *Nucl. Phys.* **B259**, 702 (1985) [Erratum, *Nucl. Phys.* **B263**, 746 (1986)].
- [53] M. Diehl, P. Kroll, C. Vogt, *Eur. Phys. J.* **C26**, 567 (2003) [[hep-ph/0206288](#)].
- [54] C.F. Berger, W. Schweiger, *Eur. Phys. J.* **C28**, 249 (2003) [[hep-ph/0212066](#)].
- [55] P.V. Pobylitsa, M.V. Polyakov, M. Strikman, *Phys. Rev. Lett.* **87**, 022001 (2001) [[hep-ph/0101279](#)].
- [56] S.J. Brodsky, G.P. Lepage, P.B. Mackenzie, *Phys. Rev.* **D28**, 228 (1983).
- [57] S.J. Brodsky, M.S. Gill, M. Melles, J. Rathsmann, *Phys. Rev.* **D58**, 116006 (1998) [[hep-ph/9801330](#)].
- [58] S.J. Brodsky, M. Melles, J. Rathsmann, *Phys. Rev.* **D60**, 096006 (1999) [[hep-ph/9906324](#)].
- [59] S.J. Brodsky, G.T. Gabadadze, A.L. Kataev, H.J. Lu, SLAC-REPRINT-1995-004.
- [60] M.R. Pennington, [hep-ph/0009267](#).
- [61] D. Mueller, D. Robaschik, B. Geyer, (Leipzig U.), in B. Geyer, (ed.) *et al.*, *Quantum Physics and Condensed Matter Physics*, 1992, p. 102–109.
- [62] M. Diehl, *Nucl. Phys. Proc. Suppl.* **126**, 271 (2004) [[hep-ph/0306311](#)].
- [63] S.J. Brodsky, T. Kinoshita, H. Terazawa, *Phys. Rev.* **D4**, 1532 (1971).
- [64] M. Diehl, T. Gousset, B. Pire, [hep-ph/0010182](#).
- [65] S.J. Brodsky, F.E. Close, J.F. Gunion, *Phys. Rev.* **D5**, 1384 (1972).